ChemComm

COMMUNICATION

View Article Online
View Journal | View Issue

Cite this: *Chem. Commun.*, 2026, **62**, 2981

Received 30th November 2025,
Accepted 4th January 2026

DOI: 10.1039/d5cc06802a

rsc.li/chemcomm

A 2nd-generation scalable synthesis of the HIV-1 entry inhibitor CJF-III-288 enabled by photoredox catalysis

Jonathan W. Nadraws, *[a] Maithili S. Pokle†[b] and Amos B. Smith III[c]

The development and optimization of a 2nd-Generation process synthesis for the human immunodeficiency virus-1 entry inhibitor CJF-III-288 bis-trifloroacetate salt 1 is reported. The route eliminates the use of noble metals, decreases the step count nearly by half, and increases the overall yield tenfold.

As of 2023, 39.9 million people worldwide were living with the human immunodeficiency virus (HIV), with 1.3 million new infections that year alone.[1] HIV infection without treatment leads to acquired immunodeficiency syndrome (AIDS), a range of conditions that weaken the immune system thereby increasing the risk of acquiring other common and/or opportunistic infections, greatly reducing life-expectancy.[2] The highly active antiretroviral therapy (HAART) regimen results in almost total restoration of normal immune function and a normal lifespan, but does not eliminate viral reservoirs, necessitating lifelong adherence to treatment.[3] Thus, in order to end the HIV epidemic, curative treatment is needed.

Targeting the viral envelope glycoprotein (Env), the only virus-specific protein on the surface of virus particles and infected cells, comprises a selective tactic to block the viral entry process and target the viral reservoir.[4] CD4-mimetic compounds (CD4mcs) developed in the Smith Group bind to Env and expose gp120 epitopes recognized by otherwise "non-neutralizing" antibodies, blocking viral entry and allowing the neutralization of infectious HIV-1 virus particles. Our lead CD4mc **CJF-III-288** displays promising low micromolar activity against many primary strains of HIV-1 and enhances binding of HIV+ plasma to HIV infected cells and increases HIV+ plasma mediated antibody-dependent cellular cytotoxicity (ADCC) compared to previous generations of CD4mc.[4] These results justified the development of a more efficient synthesis of **CJF-III-288** to access larger quantities of the compound to facilitate animal studies. The established route to synthesize **CJF-III-288**, developed initially to enable structure–activity relationship (SAR) studies of the indoline CD4mcs, is a laborious and time-consuming 18 steps long, with 11 flash column purifications and an overall yield of 0.3% (Fig. 1).[4] The use of noble and toxic metals, such as osmium, palladium, and tin, is also undesirable from a cost and safety standpoint, and triphosgene's use poses a significant safety hazard in the lab when used on scale. The length derives from protecting group and functional group manipulations, and the reliance on two-electron transformations for installing the amine functionality. The need to build up negative charge at the transmetalating carbon of the alpha-amino coupling partners may lead to poor reactivity; the same is true for the corresponding Michael addition donors.[5] Additionally, these reactions often require harsh nucleophiles and bases that pose issues for functional group sensitivity. Alternatively, alpha-amino radicals have seen extensive use in photoredox catalysis as their high stability and nucleophilicity

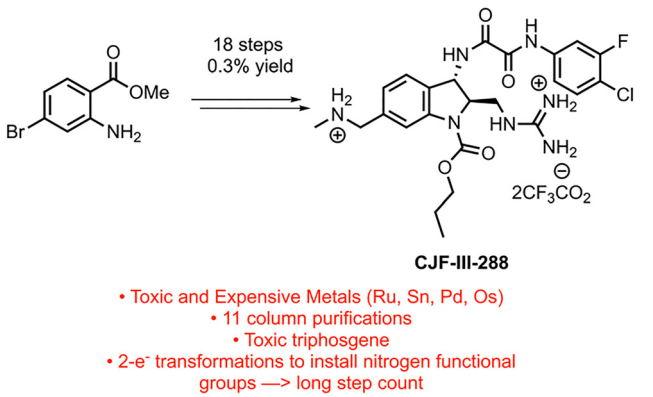

Fig. 1 1st-generation synthesis.

[a] *Department of Chemistry, University of Pennsylvania, 231 South 34th St, Philadelphia, Pennsylvania, 19104, USA. E-mail: jnadraws@sas.upenn.edu*
[b] *Maithili S. Pokle – Department of Chemistry, University of Pennsylvania, 231 South 34th St, Philadelphia, Pennsylvania, 19104, USA. E-mail: mapokle@sas.upenn.edu*
[c] *Department of Chemistry, University of Pennsylvania, 231 South 34th St, Philadelphia, Pennsylvania, 19104, USA. E-mail: smithab@sas.upenn.edu*
† Current address: Department of Chemistry, Scripps Research, La Jolla, California 92037, USA; mpokle@scripps.edu

makes them useful reagents in a variety of reactions.[6] Radical chemistry is also generally more functional group tolerant and avoids many of the substrate sensitivity issues seen in two electron chemistry.

The methylamino methyl side chain and methyl guanidine substituent were identified as areas where the implementation of photoredox chemistry would lead to significant improvements in the efficiency of the route. The 2nd-generation retrosynthesis of **CJF-III-288** begins with late-stage introduction of the aryl oxalamide moiety *via* amidation of amine **2**, which in turn could be prepared *via* Curtius rearrangement from carboxylic acid **3** (Scheme 1). Installation of the methylamino methyl side chain was envisioned using Nickel/photoredox dual catalysis with aryl bromide **4** as the electrophile. Diastereoselective Giese addition into Michael acceptor **5** with judicious choice of chiral auxiliary (X) was proposed to set the stereogenicity of the 2 and 3 positions of the indoline core and install the guanidine motif in one step. Early stage carbamylation would obviate the need to swap out the carbamate group at a later stage, as in the 1st-generation synthesis. Finally, an early stage Vilsmeier–Haack formylation would be implemented to install the carbonyl group at the 3 position of the indoline core, beginning from commercially available 6-bromoindole **6**.

Investigation of a 2nd-generation synthesis of **CJF-III-288** begins with Vilsmeier–Haack formylation of **6** (Scheme 2), which proceeds in near quantitative yield on 105-gram scale.[7] An earlier attempt to convert **6** directly to the carboxylic acid was unsuccessful, as the resulting acid lacked enough solubility in common organic solvents to make it useful for further

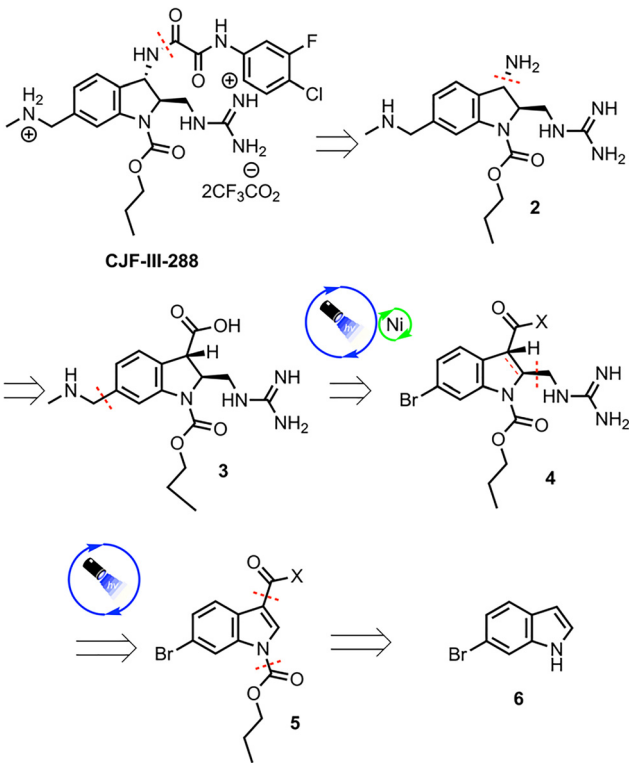

Scheme 1 Retrosynthesis of **CJF-III-288**.

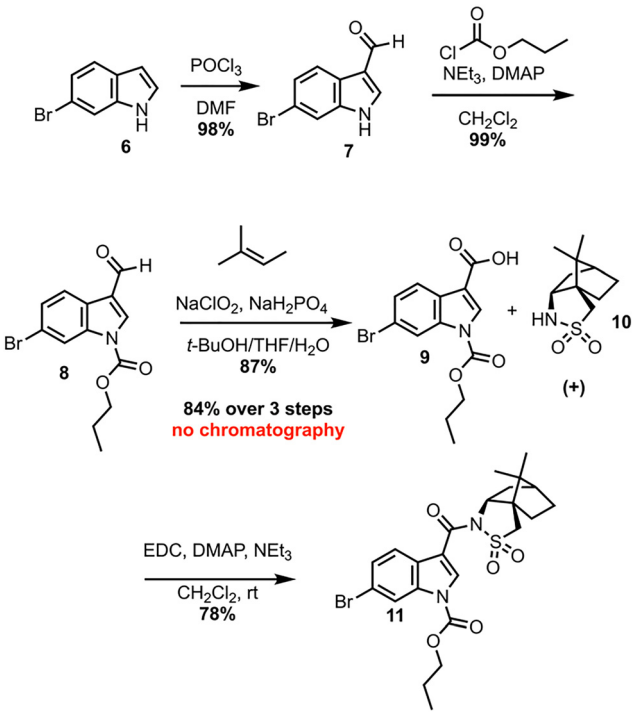

Scheme 2 Early-stage synthesis of **CJF-III-288**.

chemistry. Carbamylation of **7** with propyl chloroformate then furnishes propyl carbamate **8**, again in excellent yield on nearly an 80-gram scale. A Pinnick oxidation of aldehyde **8** next leads to carboxylic acid **9** in an excellent 87% yield on a 91-gram scale.[8] These first three steps proceed without silica-gel chromatography or recrystallization in an overall 84% yield. Acid **9** serves as the coupling partner with the commercially available, inexpensive (+)-camphorsultam **10** to yield **11** in 78% yield after silica-gel chromatography. The resulting amide **11** was envisioned as a Giese acceptor in a photoredox Giese addition using a guanidine-based radical donor.

The dearomatization of indoles bearing a champhorsultam moiety as a chiral auxiliary is established chemistry, with high diastereoselectivities observed in previous investigations.[9] Hydrogen atom transfer (HAT) catalysis was selected for its good atom economy, operational simplicity, and the ease by which the C–H radical precursors can be accessed (Scheme 3). Investigations began with globally protected precursor **12** to minimize potentially reactive guanidine nitrogen sites. HAT catalysts are chemical species that abstract homolytically labile hydrogen atoms from molecules. Under numerous protocols employing HAT catalysts and catalytic systems, such as Eosin Y, the "push–pull" benzophenone catalyst 4-Methoxy-4′-trifluoromethylbenzophenone and copper cocatalyst, and a dual catalytic system employing iridium and quinuclidine catalysts, no formation of the adduct **13** was observed.[10–12] A prohibitively large C–H bond dissociation energy (BDE) of **12**, or diminished nucleophilicity (due to either enhanced stability or steric hindrance) of the corresponding radical, was hypothesized as potential reasons for the lack of reactivity.

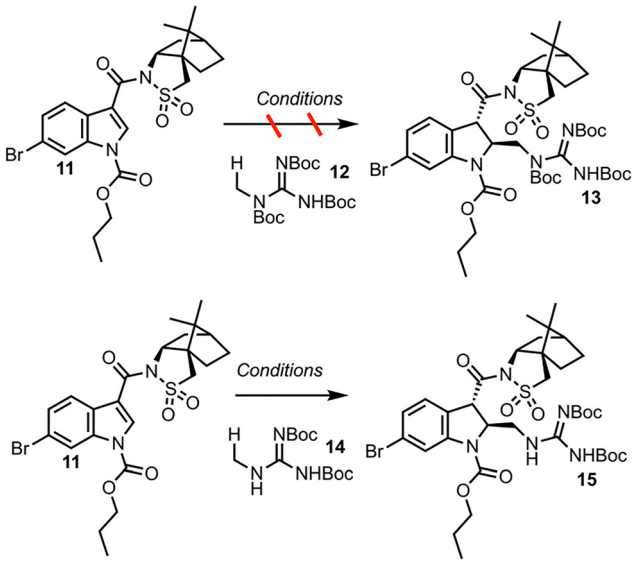

Scheme 3 Investigation of the Giese addition.

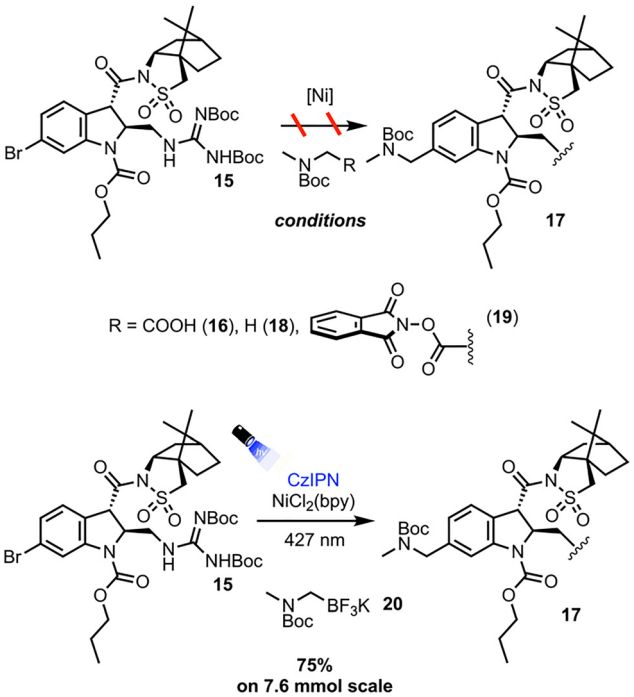

Scheme 4 Investigation of the cross-coupling.

Consequently, precursor **14**, with no *tert*-butoxycarbonyl (Boc) group at the nitrogen alpha to the reactive center, was employed for further investigations. Utilizing tetrabutylammonium decatungstate (TBADT) as the HAT catalyst, the desired Giese adduct **15** was observed by liquid chromatography-mass spectrometry (LC-MS) analysis, in low conversion. After additional optimization, the Giese adduct **15** was isolated in a good yield of 59% with 10.4 : 1 *trans* : *cis* diastereoselectivity, and the absolute stereochemistry was confirmed by X-ray crystallography (see SI). The reaction can be performed in up to 60.3 mmol scale in batch, and the TBADT catalyst can be synthesized in house on multi-gram scale for less than a dollar per gram. Discussion of the optimization of the Giese addition may be found in the SI.

Numerous protocols exist for the dual photoredox/Ni catalyzed cross coupling of alpha-amino bearing coupling partners and aryl halides. The protocols first investigated were those employing the most easily synthetically accessible alpha-amino radical precursors (Scheme 4). With **15** as the aryl halide coupling partner, Dual Ir/Ni catalysis with Boc sarcosine **16** afforded only decomposition of the starting materials and none of the desired product **17**.[13] A HAT protocol employing 4-methoxy-4′-trifluoromethylbenzophenone and Boc dimethylamine **18** afforded the desired cross-coupling adduct **17** as observed by LC-MS analysis, albeit in low conversion, likely due to the poor photo physics of the benzophenone triplet state sensitizers.[14] To remedy this, protocols and radical precursors that would lead to more efficient generation of the desired alpha amino radical were sought out. Employing redox-active ester **19** in a net-reductive cross coupling protocol with stoichiometric photoreductant Hantzsch ester affords **17** in 13% yield on 2 mmol scale.[15] While an appreciable amount of the desired product was obtained, the yield was low due to a largely inefficient reaction producing significant protodehalogenation side product and leaving a significant amount of unreacted starting material. The net-reductive reaction conditions and rapid fragmentation of **19** likely leads to fast generation of the corresponding alpha amino radical, but in the absence of an appreciable amount of oxidative addition complex, non-productive processes such as radical quenching and ultimately protodehalogenation of **15** predominate. The solution was to employ a net-neutral process where the build-up of reactive intermediates could be minimized. Thus, employing CzIPN as the organic photocatalyst and (2,2′-bipyridine)nickel dichloride ($NiCl_2$(bpy)), along with trifluoroborate precursor **20**, the desired adduct **17** was obtained in 75% yield after flash column chromatography on 7.6 mmol scale.[16] Discussion of the optimization of the cross-coupling may be found in the SI.

The final synthetic challenge left to be overcome in the 2nd-generation synthesis of **CJF-III-288** was the conversion of the carbonyl group at position 3 of the indoline to the primary amine **21** (Scheme 5). Applying Curtius conditions to **17** with treatment with diphenyl phosphoryl azide (DPPA) under refluxing conditions, instead of resulting in intermolecular capture of the resulting phosphate ester with azide to afford acyl azide, results in intramolecular capture by the guanidine moiety to give **22**. The solution was to employ a reaction mechanistically analogous to the Curtius rearrangement but proceeding through less electrophilic intermediates, the lesser known Lössen rearrangement.[17] Aminolysis of **17** with hydroxylamine furnishes hydroxamic acid **23**. Compound **23** is used in a self-propagative, "pseudo-catalytic" Lössen rearrangement, wherein condensation with acetonitrile first occurs to activate the substrate *in situ*, which undergoes rearrangement to isocyanate **24**. Compound **24** is either hydrolyzed, or enters the self-propagative catalytic cycle with another equivalent of **23** to

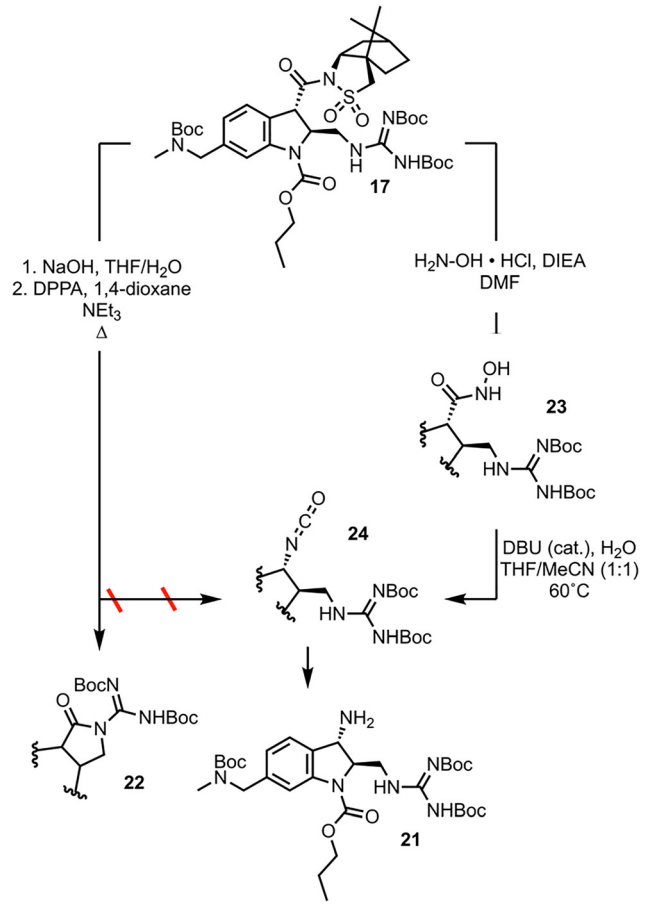

Scheme 5 Development of the late-stage synthesis.

afford primary amine **21**. Data detailing the optimization of these two transformations is found in the SI.

The synthesis was completed by coupling of the *meta*-fluoro-*para*-chloro acid **25** to amine **21** using propanephosphonic acid anhydride (T3P), effective for sterically encumbered substrates on large scale (Scheme 6).[18,19] Global Boc deprotection of **26** with TFA yields **CJF-III-288** in nearly quantitative yield. The synthesis was further validated by scaling up the cross coupling of **15** and **20**, which can be performed on a 33.16 mmol scale in a single batch. The sequence from intermediate **15** to **26** was performed on a 79 mmol scale, affording 5.66 grams of **26** after a single flash column purification. The global Boc deprotection yielded 4.90 grams of **1**.

In summary, the 2nd-generation synthesis of **CJF-III-288**, beginning on over a hundred-gram scale, proceeds in 10 steps to yield **1** in an overall yield of 3%. This reduces the step count almost by half compared to the original of 18 steps, and the overall yield has increased tenfold compared to the original yield of 0.3%. This was achieved by reducing the step count of the installation of the guanidine group and stereochemistry from 5 steps to 1 step, and of the methylamino methyl group from 3 steps to 1 step, compared to the first-generation synthesis. The route has been used to synthesize 5.7 grams of **1**, which are currently being used in *in vivo* biological studies to determine the efficacy of **CJF-III-288** to prevent and cure HIV

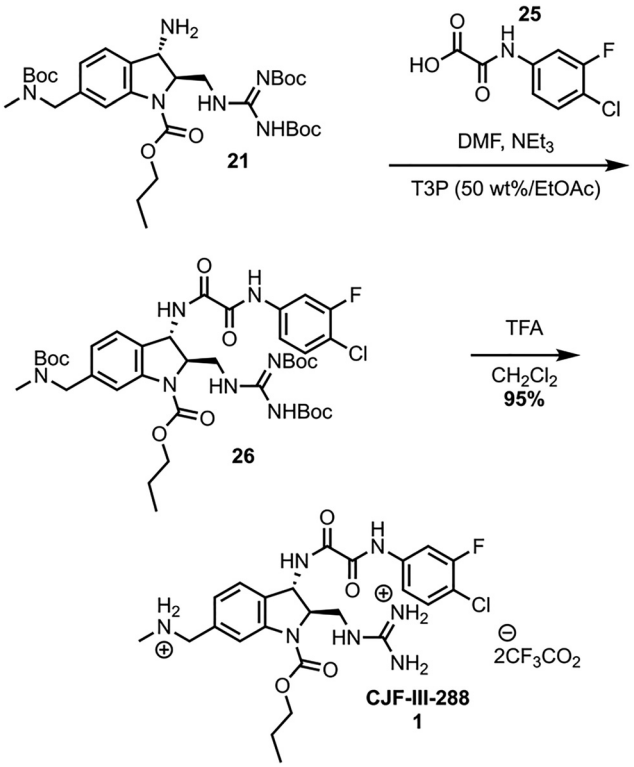

Scheme 6 Endgame synthesis.

infection in monkey models. Additionally, the photochemistry developed for the synthesis holds promise for use in further analogue synthesis. The modular nature of both reactions allows incorporation of diverse alkyl, aryl, methylamino, and methyloxy functionality at both the 2 and 6 positions of the indoline core and further optimization of the potency and physicochemical properties of the indole CD4mcs.

Conflicts of interest

There are no conflicts to declare.

Data availability

The data underlying this study, including experimental procedures, characterization data, ^{1}H-NMR/^{13}C-NMR spectra, and crystal structures are available in the supplementary information (SI). Supplementary information is available. See DOI: https://doi.org/10.1039/d5cc06802a.

Raw FID data is openly available in Dryad Databank at DOI: https://doi.org/10.5061/dryad.4b8gthtsf.

CCDC 2484437 contains the supplementary crystallographic data for this paper.[20]

Acknowledgements

Financial support was provided by the National Institutes of Health through grants NIH-1R01AI176904-01A1, NIH 1R01AI174908-01A1,

NIH 1UM1AI164562, and NIH 5P01AI150471. Instrumentation supported by the NSF Major Research Instrumentation Program (award NSF CHE-1827457) and Vagelos Institute for Energy Science and Technology were used in this study. We thank Borna Saeednia at the University of Pennsylvania for assistance with HRMS analysis and Dr's Jun Gu and Chad Lawrence for assistance with NMR analysis. We thank Dr's Mark Campbell, David Fialho, Viktor Polites, Christopher Fritschi, and Robert Micikas for their helpful comments and insights.

References

1 https://unaids.org/sites/default/files/media_asset/UNAIDS_FactSheet_en.pdf (accessed 2025-05-18).
2 M. K. Powell, K. Benková, P. Selinger, M. Dogoši, I. Kinkorová Luňáčková, H. Koutníková, J. Laštíková, A. Roubíčková, Z. Špůrková and L. Laclová, *et al.*, *PLoS One*, 2016, **11**, e0162704.
3 C. Katlama, S. G. Deeks, B. Autran, J. Martinez-Picado, J. van Lunzen, C. Rouzioux, M. Miller, S. Vella, J. E. Schmitz and J. Ahlers, *et al.*, *Lancet*, 2013, **381**, 2109–2117.
4 C. J. Fritschi, S. Anang, Z. Gong, M. Mohammadi, J. Richard, C. Bourassa, K. T. Severino, H. Richter, D. Yang and H.-C. Chen, *et al.*, *Proc. Natl. Acad. Sci. U. S. A.*, 2023, 120.
5 S. Roediger, E. Le Saux, P. Boehm and B. Morandi, *Nature*, 2024, **636**, 108–114.
6 K. Nakajima, Y. Miyake and Y. Nishibayashi, *Acc. Chem. Res.*, 2016, **49**, 1946–1956.
7 Sl Dominique, P. Weiß, J. Ermert, J. C. Meleán, F. Zarrad and B. Neumaier, *Eur. J. Org. Chem.*, 2016, 4621–4628; Y. Gao, S. Osman and K. Koide, *ACS Med. Chem. Lett.*, 2014, **5**, 863–867.
8 E. Dalcanale and F. Montanari, *J. Org. Chem.*, 1986, **51**, 567–569.
9 Y. Zhang, P. Ji, F. Gao, H. Huang, F. Zeng and W. Wang, *ACS Catal.*, 2021, **11**, 998–1007.
10 X. Z. Fan, J. W. Rong, H. L. Wu, Q. Zhou, H. P. Deng, J. Da Tan, C. W. Xue, L. Z. Wu, H. R. Tao and J. Wu, *Angew. Chem., Int. Ed.*, 2018, **57**, 8514–8518.
11 B. Abadie, D. Jardel, G. Pozzi, P. Toullec and J.-M. Vincent, *Chemistry*, 2019, **25**, 16120–16127.
12 V. Dimakos, H. Y. Su, G. E. Garrett and M. S. Taylor, *J. Am. Chem. Soc.*, 2019, **14**, 5149–5153.
13 Z. Zuo, D. T. Ahneman, L. Chu, J. A. Terrett, A. G. Doyle and D. W. C. MacMillan, *Science*, 2014, **345**, 437–440.
14 Y. Shen, Y. Gu and R. Martin, *J. Am. Chem. Soc.*, 2018, **140**, 12200–12209.
15 L. M. Kammer, S. O. Badir, R.-M. Hu and G. A. Molander, *Chem. Sci.*, 2021, **12**, 5450–5457.
16 J. C. Tellis, D. N. Primer and G. A. Molander, *Science*, 2014, **345**, 433–436.
17 N. A. Strotman, A. Ortiz, S. A. Savage, C. R. Wilbert, S. Ayers and S. Kiau, *J. Org. Chem.*, 2017, **82**, 4044–4049.
18 J. R. Dunetz, Y. Xiang, A. Baldwin and J. Ringling, *Org. Lett.*, 2011, **13**, 5048–5051.
19 A. Mattellone, D. Corbisiero, L. Ferrazzano, P. Cantelmi, G. Martelli, C. Palladino, A. Tolomelli and W. Cabri, *Green Chem.*, 2023, **25**, 2563–2571.
20 CCDC 2484437: Experimental Crystal Structure Determination, 2026, DOI: 10.5517/ccdc.csd.cc2pd84j.